Chemical Geology 609 (2022) 121048

Contents lists available at ScienceDirect

Chemical Geology

journal homepage: www.elsevier.com/locate/chemgeo

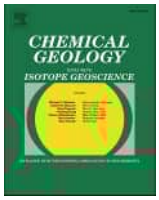

# Geochemical and geophysical effects of tectonic activity in faulted areas of the North China Craton

Zhi Chen [a,*], Ying Li [a,*], Zhaofei Liu [a], Hongyi He [a], Giovanni Martinelli [b], Chang Lu [a], Zihan Gao [a]

[a] CEA key Laboratory of Earthquake Prediction, Institute of Earthquake Forecasting, Beijing 100036, China
[b] INGV-National Institute of Geophysics and Volcanology Dept. of Palermo, Palermo 90146, Italy

ARTICLE INFO

Editor: Dr Don Porcelli

*Keywords:*
Fluid geochemistry
Tectonic activity
North China Craton
Northeastern Tibetan Plateau
Zhang-Bo seismic zone

ABSTRACT

Fluid geochemistry in active fault zones has been proven to be sensitive to tectonic activity. The North China Craton (NCC) has attracted much attention because of its complex and intense tectonic activity. In this study, fluid geochemistry in the primary active fault zones in the NCC was investigated, including inference of its tectonic activity. Stronger degassing from soil and springs has been observed in the northeastern Tibetan Plateau (NETP) and the Zhang-Bo seismic zone (ZBSZ) than in the other seismic zones. Both geological soil gas and deep-derived gas (crust- or mantle-derived gas) from springs were concentrated there. Also, a comprehensive analysis has indicated that the development of new fractures might have occurred widely beneath the NETP and ZBSZ because of the strong regional tectonic activity there. The $^{3}He/^{4}He$ and $^{4}He/^{20}Ne$ of gas from the springs in the ZBSZ suggest that the low-velocity zone 20– 40 km deep might be a magmatic intrusion derived from the mantle. However, crust-derived gas accompanied with a negligible mantle-derived component has been detected in the Diebu-Bailongjiang fault (DBF), the West Qinling fault (WQLF), and the Liupanshan fault (LPSF) in the NETP. There, the occurrence of more new fractures was probable, in accordance with the obvious $\delta^{18}O$ shift of the water from the springs in the fault zones. This suggests that a channel flow, also depicted by the low-velocity zone 20–40 km deep, could have formed within the crust and that the probable leading front reached the LPSF.

## 1. Introduction

The NCC was formed about 1.85 Ga ago and has attracted much attention because of its dramatic tectonic activity and complex geochemical characteristics of fluid trapped in the basement rocks and degassing within the fault zones (Chen and Ai, 2009; Chen et al., 2018). The NCC was destroyed in the Late Mesozoic subject to the combined action of collision between the North China and Yangtze blocks and subduction westward of the paleo-Pacific plate (Zhu et al., 2012), according to numerous previous studies focusing on regional magmatism, tectonic deformation and lithospheric structure (Zheng et al., 2009; Zhai and Santosh, 2013), and became active and presented regional rotation within the plate since the Early Cretaceous (Wu et al., 2005), which contradicted the classical plate tectonic theory stating that the stability was an inherent property of Craton (Perchuk et al., 2020). Additionally, significant differences in lithospheric structure and tectonic activity between the eastern and western segments of the NCC emerged after the destruction of the NCC (Chen et al., 2014). Attributed to the weak extensional deformation in the Early Cretaceous (Zhai and Liu, 2003; Zhai, 2019), the western segment of the NCC presented a framework of huge basins, where depression or fracture-depression occurred, and volcanism and tectonic activity were not active there, indicating its stability properties (Zhu et al., 2012), while the eastern segment was active, where ductile tectonic deformation, crustal remelting, weakening, thinning and extension, and low velocity within the lithosphere were occurred extensively (Zheng et al., 2015). Its tectonic state was variable (Zhao et al., 2017), volcanism with high-K calc-alkaline magma was drastic there in the Early Cretaceous, while it quietened down in the Cenozoic (Chen et al., 2005). Therefore, further implementation of active state investigation for the NCC is needed, which could be of great significance and essential for understanding and establishing a new continental evolution theory.

Earth is an open system, and fluid release is a major means of exchanging matter and energy at various depths (Tao, 2005). An active fault system and its associated fracturing play a fundamental role in deep fluids such as $CO_2$, Rn, and He ascending toward the surface by creating pathways that extend from the deep lithosphere to the earth's surface. Deep fluids can migrate upward through those pathways

* Corresponding authors.
*E-mail addresses:* dugu_830822@163.com (Z. Chen), subduction6@hotmail.com (Y. Li).

https://doi.org/10.1016/j.chemgeo.2022.121048
Received 15 February 2022; Received in revised form 16 July 2022; Accepted 2 August 2022
Available online 6 August 2022

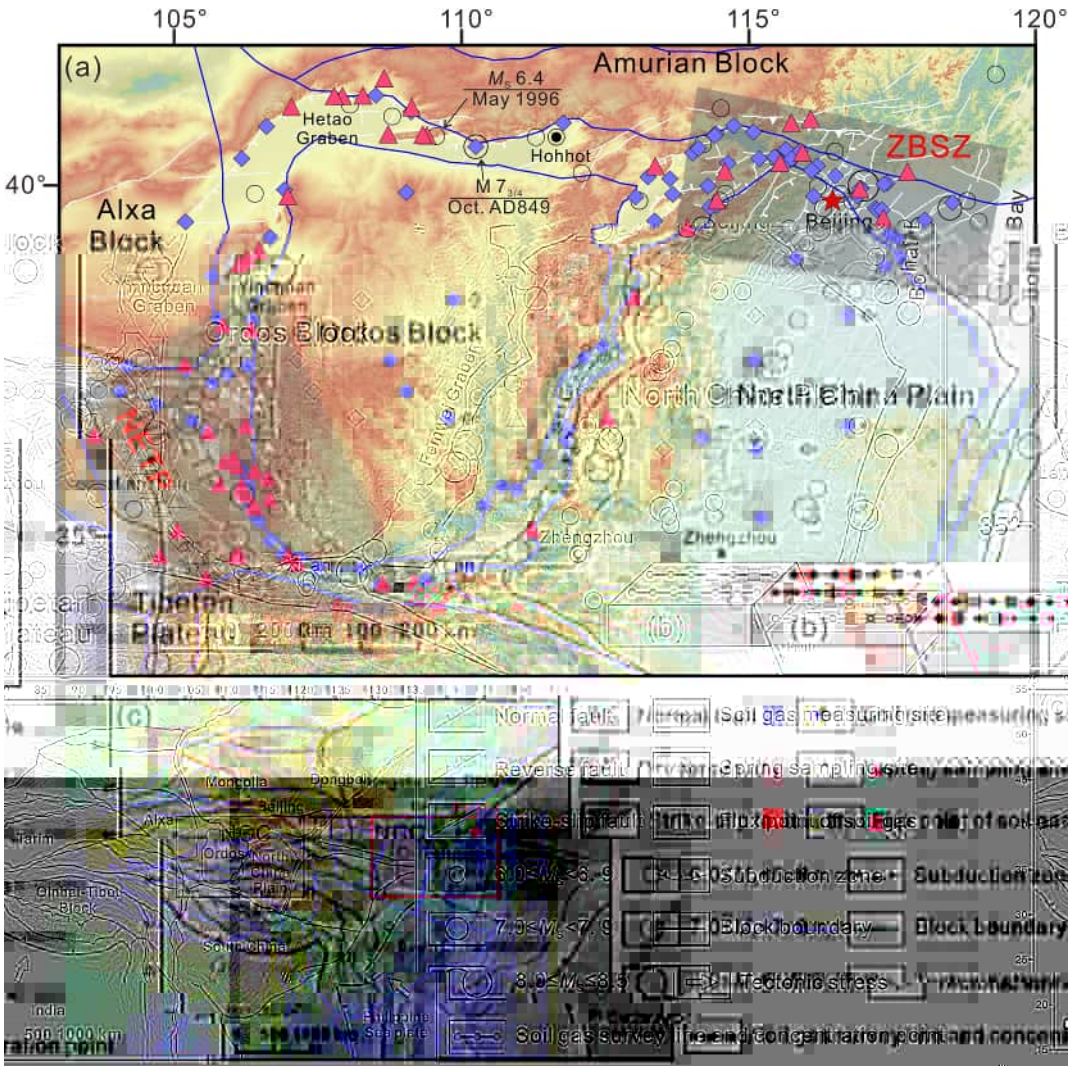


**Fig. 1.** Regional map of the study area. (a) shows the geological setting and measuring sites in the study area, (b) shows the layout of soil gas survey line, concentration and flux measuring points, (c) shows the location of the study region in China. Earthquakes were recorded from 780 BCE to 2020 (http://news.ceic.ac.cn).

because of their enhanced permeability and porosity relative to unfractured rock, and those fluids can carry specific geochemical information about the physicochemical evolution in the deep lithosphere (Yuce et al., 2014; D'Alessandro et al., 2020; Chen et al., 2019; Zhang et al., 2021).

Numerous field investigations have provided evidence that observing the geochemical characteristics of fluid emissions from the fault zone could be a potential proxy for investigation of physicochemical evolution in the lithosphere (Bedrosian et al., 2004; Faulkner et al., 2010; Yuce et al., 2017), which has made a significant contribution to the evaluation of mineral resources and modeling of geothermal water circulation (Pang et al., 2018), monitoring of geodynamic processes, revealing hidden faults, monitoring fault activity (Bonforte et al., 2013; Yuce et al., 2017; Yang et al., 2018), investigating strain accumulation and tectonic destruction (Bonforte et al., 2013; Chen et al., 2015), monitoring volcanic activity (Neri et al., 2016), monitoring seismic activity (Martinelli and Tamburello, 2020), and earth degassing investigation (Chen et al., 2018; Tamburello et al., 2018). Also, extensive laboratory experiments have been conducted concerning gas emission during rock failure and geochemical variations in the process of water-rock interactions under crustal conditions (Koike et al., 2015; Sun et al., 2016a). They have offered an experimental and physical basis for monitoring characteristic geochemical variation in the tectonic zone, which could provide information about the geodynamic processes in the deep earth (Roeloffs, 1999; Girault et al., 2017).

Fluid geochemistry investigations had been widely implemented in the Cratons to study the destruction, regional tectonic activities, and mechanism of fluid genesis and transportation (Crossey et al., 2009; Shen et al., 2013; Zhang et al., 2016; Muirhead et al., 2020). Combined with isotope correlation diagrams, the noble gas isotopes in corundum and peridotite xenoliths provided unique and important constraints for comprehensive refertilization of lithospheric mantle in the eastern North China Craton (He et al., 2011). Xu et al. (2014) determined that the helium found in fluid collected from the crust in the Eastern Block (EB) was derived from the mantle and that active fault acted as an important pathway for mantle-derived ascending toward the surface in the nonvolcanic regions. The gas geochemistry investigation confirmed that deep fluid was active in the eastern NCC, and the degassing of mantle-derived gas could be a widespread occurrence in the EB and Trans-North China Orogen (TNCO) (Lu et al., 2021).

In this study, the distribution of geochemical characteristics of fluid within the principal active fault zones in the NCC was investigated, and the geochemical and geophysical effects of tectonic activity in faulted areas of the NCC were discussed.

## 2. Geological setting

Archean Cratons are stable tectonic units characterized by a cold,

lacles

old, and thick (approximately 200 km) lithospheric keel. They generally exhibit a low heat flow and a lack of volcanism and large earthquakes (King, 2005); examples include the Kaapvaal Craton, the North American Craton, and the Australian Craton. However, the NCC in eastern Asia is an exception. Recent studies have suggested that the eastern NCC had undergone significant lithospheric thinning and modification during the Mesozoic Cenozoic period, which was deduced by examining the physical and chemical properties of the subconti

**Table 2**
Geochemical characteristics of springs within the active fault zones in the NCC.

| Region | Number | Spring | Longitude (°E) | Latitude (°E) | δD (‰) | $\delta^{18}O$ (‰) | $^{3}He/^{4}He$ | $^{4}He/^{20}Ne$ | R/Ra | Rc/Ra | References |
|---|---|---|---|---|---|---|---|---|---|---|---|
| | **o. 1** | QL | 103.628 | 36.4552 | −82.35 | −9.12 | $1.10 \times 10^{-8}$ | 1048 | 0.01 | 0.01 | |
| | **o. 2** | SJ | 106.253 | 36.587 | −87.90 | −9.19 | $1.03 \times 10^{-7}$ | 841 | 0.07 | 0.07 | |
| | **o. 3** | SJ1 | 106.252 | 36.587 | −80.71 | −9.42 | $7.21 \times 10^{-8}$ | 1611 | 0.05 | 0.05 | |
| | **o. 4** | CSH | 106.04 | 36.131 | −79.40 | −9.80 | $9.89 \times 10^{-8}$ | 15 | 0.07 | 0.05 | This study |
| | **o.** | XKH | 106.082 | 36.019 | −75.50 | −11.74 | $3.12 \times 10^{-8}$ | 158 | 0.02 | 0.02 | |
| | **o.** | XKH1 | 106.083 | 36.018 | −76.99 | −9.41 | $1.70 \times 10^{-8}$ | 313 | 0.01 | 0.01 | |
| | **o.** | WM | 106.991 | 34.737 | −75.27 | −9.39 | $7.33 \times 10^{-7}$ | 25 | 0.02 | 0.07 | |
| | **o.** | ZMM | 106.992 | 34.736 | −74.50 | −9.44 | $1.41 \times 10^{-8}$ | 110 | 0.01 | 0.01 | |
| **ortheastern Tibetan Plateau** | **o.** | PL | 106.661 | 35.543 | – | – | $5.80 \times 10^{-7}$ | – | | | |

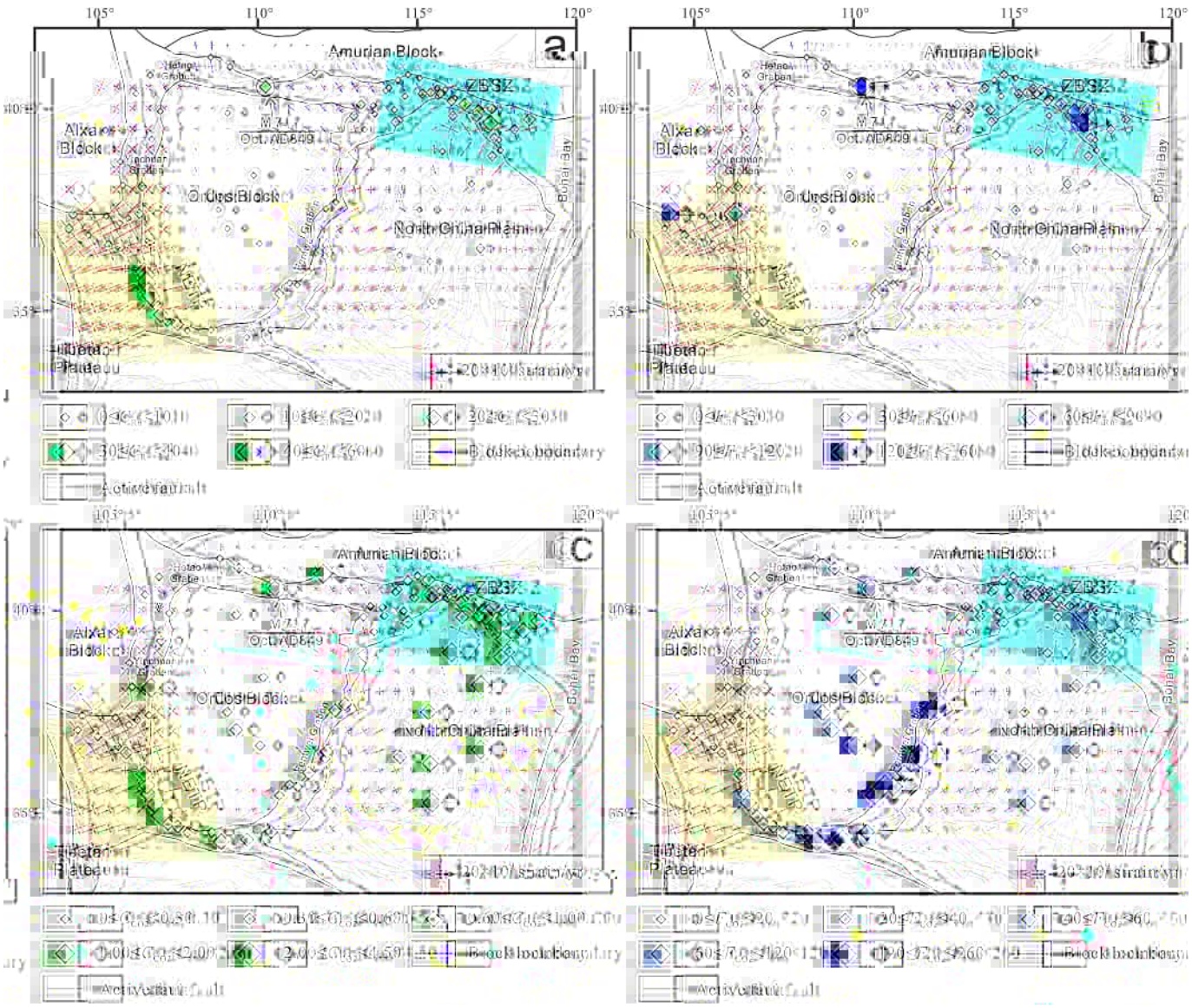


**Fig. 4.** Soil gas degassing features in the NCC. In particular: (a) Rn concentration and shear strain; (b) Rn flux and shear strain; (c) $CO_2$ concentration and shear strain; (d) $CO_2$ flux and shear strain. Shear strain data are according to Zhang et al. [2018] and Wang and Shen [2019]. The yellow zone is the ZBSZ, the blue zone is the NETP. (For interpretation of the references to colour in this figure legend, the reader is referred to the web version of this article.)

in active fault zones in the NETP and the ZBSZ (Figs. 4 and 5). The mean Rn concentration and flux from the active fault zones in the NETP (4.67– 66.34 kBq $m^{-3}$ and 0.90– 140.33 mBq $m^{-2}$ $s^{-1}$) and the ZBSZ (3.80– 37.89 kBq $m^{-3}$ and 10.25– 152.38 mBq $m^{-2}$ $s^{-1}$) were much higher than those in the other fault zones in the study area (1.60– 15.33 kBq $m^{-3}$ and 3.66– 49.82 mBq $m^{-2}$ $s^{-1}$) and the Ordos basin (0.20– 8.35 kBq $m^{-3}$ and 0.10– 26.35 mBq $m^{-2}$ $s^{-1}$). The average values of Rn concentration and flux in the NETP (23.55 kBq$m^{-3}$ and 32.69 mBq $m^{-2}$ $s^{-1}$) were 3.4 and 1.2 times as high as those in the other fault zones, except for those in the ZBSZ, and 4.4 and 1.9 times as high as those in the Ordos Basin. The average values of Rn concentration and flux in the ZBSZ (13.18 kBq$m^{-3}$ and 47.64 mBq $m^{-2}$ $s^{-1}$) were 1.9 and 1.7 times as high as those in the other fault zones, except for those in the NETP, and 2.5 and 2.7 times as high as those in the Ordos basin (Table 1). Also, a high $CO_2$ concentration and flux were observed in the NETP and the ZBSZ, although the high $CO_2$ concentration and flux were partially distributed in the other fault zone and the Ordos Basin. In particular, both concentrations and fluxes of Rn and $CO_2$ were high in the soil gas profile ADL, where significant earthquakes occurred (http://news.ceic.ac.cn), such as the Baotou $M_S$ 6.4 earthquake in May 1996 and $M_S$ 7.8 earthquake in 849 (Dong et al., 2018). Therefore, the high concentrations and fluxes of Rn and $CO_2$ in soil gas profile ADL might be attributed to the relatively high crustal permeability likely induced by strong seismic events (Chen et al., 2018).

The natural radioactive decay of $^{226}Ra$ is a unique source of soil gas $^{222}Rn$. Whereas soil gas $CO_2$ is derived from multiple sources, it primarily originates from mantle degassing, carbonate metamorphism, carbonated dissolution, the decomposition of organic matter, and soil respiration (Caudron et al., 2012; Ramnarine et al., 2012). In the $\delta^{13}C_{CO2}$ vs.$1/CO_2$ diagram, the soil gas samples plotted within the composition mixing range between the Deep (M + C) end-member and biogenic end-member (Fig. 6), in accordance with the relatively high He concentrations (7.30– 18.01 ppm) and strong relation between soil gas $CO_2$ and He concentrations (Fig. 7), geological $CO_2$ could be inferred to ascend toward the surface through the faults in the ZBSZ, which could play a role as the carrier of geological Rn and transferred it to the shallower soil gas. In the NETP, the He concentration of soil gas within the fault zones reached up to 65.30 ppm (Zhou et al., 2011), in

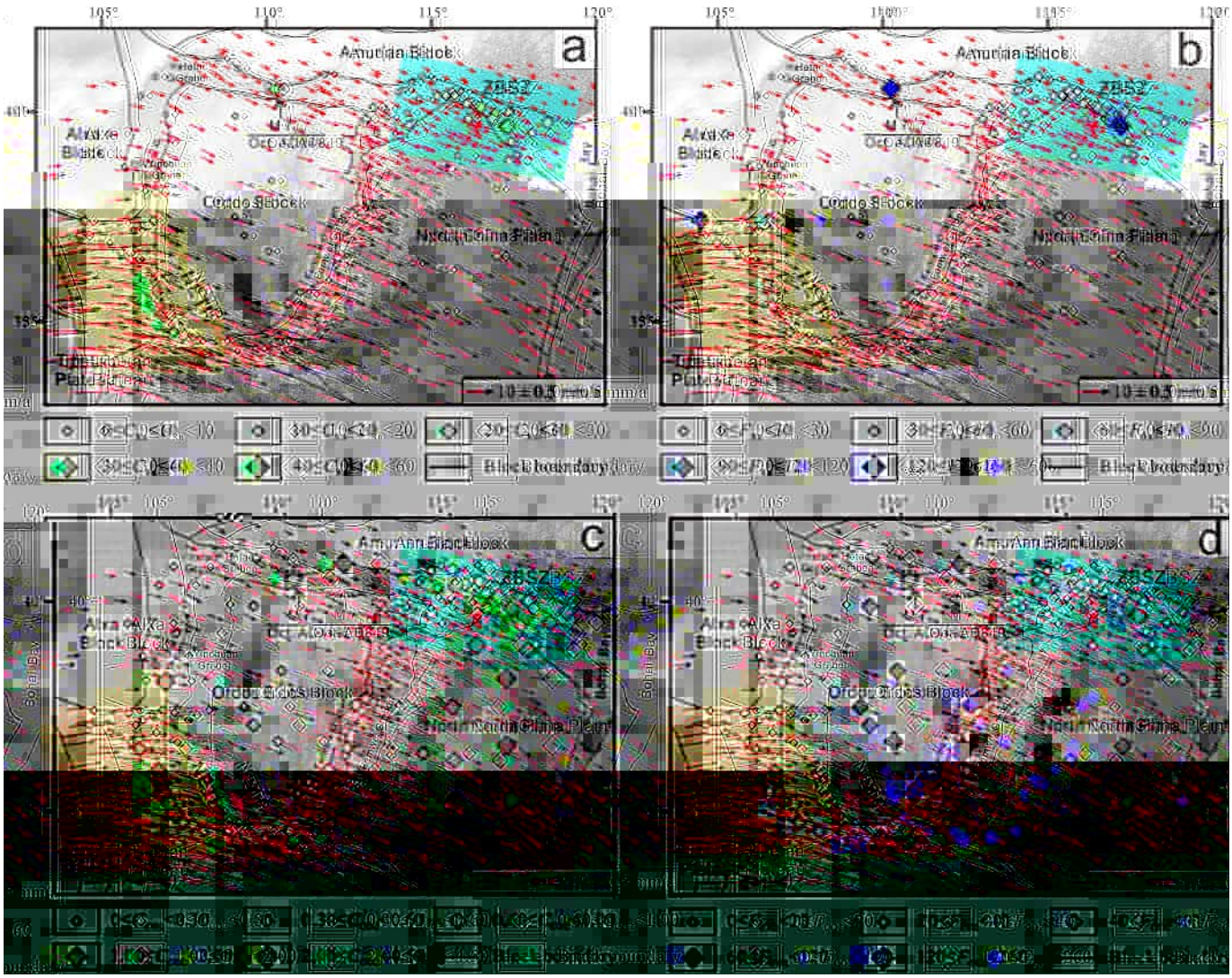


**Fig. .** The soil gas degassing features in the NCC. In particular: (a) Rn concentration and GPS velocity; (b) Rn flux and GPS velocity; (c) $CO_2$ concentration and GPS velocity; (d) $CO_2$ flux and GPS velocity. GPS velocity data are according to Zhang et al. [2018] and Wang and Shen [2019]. The yellow zone is the ZBSZ, the blue zone is the NETP. (For interpretation of the references to colour in this figure legend, the reader is referred to the web version of this article.)

accordance with the strong relationship between soil gas $CO_2$ and Rn concentrations (Fig. 7), the geological source for soil gas within the fault zones could also be inferred.

Therefore, it was apparent that the relatively high gas emissions from the fault zones, including geological gas in the soil gas and deep-derived gas (crust or mantle-derived gases) from springs, showed a concentrated distribution in the NETP and the ZBSZ. It suggested that a particular tectonic framework could be responsible for the coupled spatial distribution of gas geochemistry in the fault zones of the NCC.

### 5.2. *Tectonic framework in the NCC revealed by fluid geochemistry*

Although a coupled concentrated distribution of the degassing for geological soil gas and deep-derived gas (crust or mantle-derived gases) from springs were observed within the fault zone in the NCC, pronounced differences were still found between the isotopic ratios of gas from the springs within the NETP and those within the ZBSZ, according to the $^{3}He/^{4}He$ (R/Ra) and $^{4}He/^{20}Ne$ of gas from the springs. It seemed that abundant mantle-derived gas was degassing through the fault in the ZBSZ, while a minute amount of mantle-derived gas was degassing in the NETP (Fig. 3).

Previous research has suggested that the joint action of the India-Eurasia collision and the Pacific subduction could be a significant factor that dominated the tectonic evolution in the NCC (Chen and Ai, 2009). Due to the remote action of the India-Eurasia collision, the Tibetan Plateau moved northeastward; that movement was withstood when the Tibetan Plateau collided with the rigid Ordos block in the northeastern corner of the Tibetan Plateau. Crust shortening and over thrusting in the northeastern corner occurred (Lease et al., 2011), resulting in strong tectonic compression in the NETP margin (Fig. 1). Due to the continuous subduction and rollback of the Pacific plate, lithosphere consumption and intense lithosphere regional extension took place in the eastern NCC. This caused the eastward motion of the North China plain (Zeng et al., 2016) and obvious GPS velocity differences between the North China plain and the Amurian block, resulting in the strike-slip characteristic of the ZBSZ (Zhang et al., 2018; Wang and Shen, 2019).

In fact, extensional tectonics have been verified to facilitate fracture development, causing a stronger degassing in the normal fault zones than the thrust and strike-slip faults (Tamburello et al., 2018). Therefore, the degassing from the fault zones in the NETP and the ZBSZ should be weaker than those in the other tectonic belts in the NCC. This could be attributed to the widespread thrust and strike-slip faults in the NETP and the dominant strike-slip in the ZBSZ, whereas normal faults dominate in

the other tectonic belts (Fig. 1). Unexpectedly, relative to those in the other tectonic belts, high soil gas Rn and $CO_2$ emissions were observed (Figs. 4 and 5), and degassing in the springs only occurred in the NETP and the ZBSZ (Figs. 4 and 5).

By coincidence, an abnormally high shear strain rate and the steepest gradient of GPS horizontal velocity were also observed in the NETP and the ZBSZ (Figs. 4 and 5), The abnormal regions were roughly consistent with those where high geological soil gas (Rn, $CO_2$ and He) emission and deep-derived gas (crust or mantle-derived gases) exhalation from springs were observed (Figs. 2–5 and 7). Furthermore, it has been found in previous simulation experiments that substantially enhanced gas emissions from rocks could happen, when the differential stress on the rocks exceeded their compressive strength, resulting in the development of macroscopic fractures (new fracturing or an opening of preexisting fractures), which provides new pathways for captive gas in the rocks (Roeloffs, 1999; Girault et al., 2017). Therefore, based on the above discussion, it could be inferred that fracture development in the deep earth beneath the NETP and the ZBSZ might have occurred because of the strong regional tectonic activity there, leading to enhanced gas exhalation from the rocks in the deep earth. That might in turn have led to

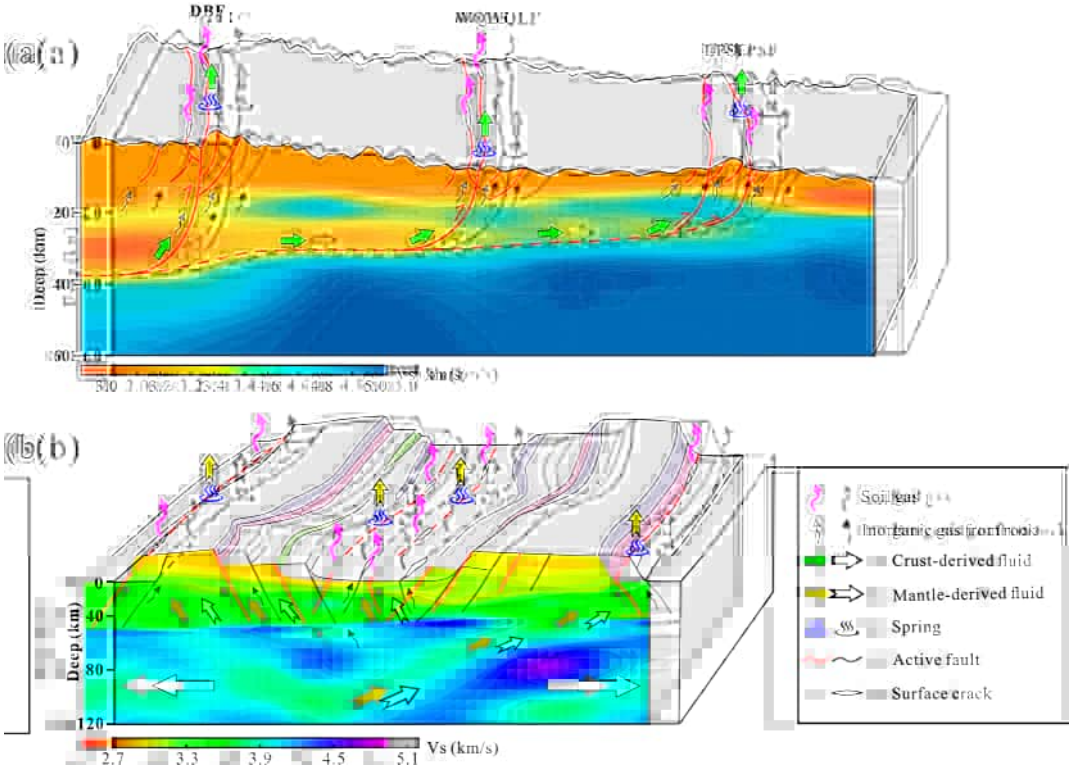


**Fig.** . Conceptual model for the difference of gas geochemistry between the NETP and the ZBSZ. (a) Conceptual model for the NETP. (b) Conceptual model for the ZBSZ. (The low-velocity zones are according to Wang et al., 2009 and Zhao et al., 2021; the fault zones are according to Jiang and Zhang, 2012 and Du et al., 2018.)

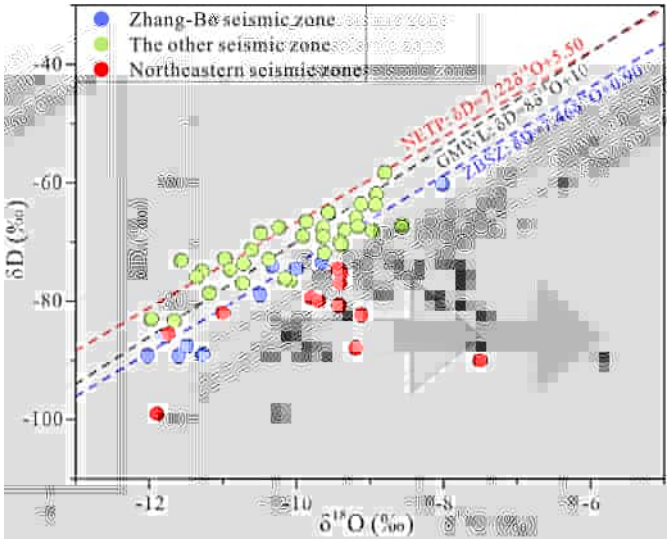


**Fig.** . δD versus $\delta^{18}O$ of water samples from the springs in the study area. GMWL stands for global meteoric water line: $\delta D = 8\ \delta^{18}O + 10$ (Craig, 1961); NETP stands for local meteoric water line in the NETP: $\delta D = 7.22\ \delta^{18}O + 5.50$ (Sun et al., 2016b); ZBSZ stands for local meteoric water line in the ZBSZ: $\delta D = 7.46\ \delta^{18}O + 0.90$ (Liu et al., 2010).

## . Conclusions

By means of a comprehensive analysis of the distribution of geochemical characteristics of fluids and geophysical characteristics within the principal active fault zones in the NCC, three conclusions can be summarized as follows:

(1) Obvious high Rn and slightly high $CO_2$ and He emissions were observed in active fault zones in the NETP, which is dominated by strong compression and thrust faults, and in the ZBSZ, which is dominated by regional extension and strike-slip fault, while Rn and $CO_2$ emissions were higher than those in the other tectonic belts with dominant extensions and normal faults in the NCC. It goes against previous research proposed that gas emissions in extensional tectonics and normal faults could be stronger than those in compression tectonics, thrust faults, and strike-slip faults.

(2) It was apparent that relatively high gas emissions from fault zones, including geological gas in soil gas and deep-derived gas (crust or mantle-derived gases) from springs, showed a concentrated distribution in the NETP and the ZBSZ. Also, an abnormally high shear strain rate and the steepest gradient of GPS horizontal velocity were both observed in the NETP and the ZBSZ. This suggests that fractures in the deep earth beneath the NETP and the ZBSZ might have developed under the strong regional tectonic activity there. This might have resulted in greater contributions of geological soil gas and deep-derived gas from springs in the NETP and the ZBSZ than those presented in the other seismic zones.

(3) The comprehensive analysis confirmed the mantle-derived intrusion into the crust beneath the ZBSZ, and the development of new fractures within the fault zone could have facilitated the migration of trapped mantle-derived gas in the ZBSZ. However, the channel flow beneath the NETP, shown by the low-velocity zone 20 to 40 km deep, intersected by deep-cut faults, could have formed within the crust, since negligible mantle-derived gas was detected in the springs in the NETP, even if more new fractures have been proved to be developed there.

(4) Based on the distribution of the geochemical characteristics of the fluid within the principal active fault zones in the NCC, it could be inferred that stronger regional tectonic activity might have occurred in the NETP and the ZBSZ than the other seismic zones, which suggested that more attention should be paid to the potential of future seismogenesis in the NETP and ZBSZ, and gas geochemistry could be a preferential method for monitoring regional tectonic and seismic activity.

## eclaration o Competing Interest

None.

## ata a ailability

All the data have been deposited in Mendeley Data repository (Mendeley Data, V2, doi: 10.17632/5bnvwxmtv8.2).

## ckno ledgements

This study was jointly supported by the National Key Research and Development Program of China (No. 2019YFC1509203), Natural Science Foundation of China (Nos. 41402298, 42073063), the Basic Science Research Plan of the Institute of Earthquake Science, China Earthquake Administration (No.2020IEF0704, 2021IEF0707, and 2021IEF1205), this work is a contribution to IGCP Project 724. Research data associated with this article had been uploaded to Mendeley Data (https://data.mendeley.com/drafts/k7xtf85nr2). All the data have been deposited in Mendeley Data repository (Chen, Zhi (2022), "Tectonic features of the Tibetan Plateau–Ordos Block

isotope geochemistry and implications for the destruction of the North China Craton. Lithos 156–159, 218–229. https://doi.org/10.1016/j.Lithos.2012.11.003.
Skelton, A., Andrén, M., Kristmannsdóttir, H., Stockmann, G., Mörth, C.M., Sveinbjörnsdóttir, Á., Jónsson, S., Sturkell, E., Guðrúnardóttir, H.R., Hjartarson, H., Siegmund, H., Kockum, I., 2014. Changes in groundwater chemistry before two consecutive earthquakes in Iceland. Nat. Geosci. 7 (10), 752–756. https://doi.org/10.1038/ngeo2250.
Sun, Q., Zhao, C., Lü, H., 2016a. Radon emission evolution and rock failure. Acta Geod. Geophys. 51 (3), 583–595. https://doi.org/10.1007/s40328-015-0147-z.
Sun, X., Wang, G., Shao, Z., Si, X., 2016b. Geochemical characteristics of emergent gas and groundwater in Haiyuan fault zone. Earth Sci. Front. 23 (3), 140–150. https://doi.org/10.13745/j.esf.2016.03.018 (in Chinese with an English abstract).
Tamburello, G., Pondrelli, S., Chiodini, G., Rouwet, D., 2018. Global-scale control of extensional tectonics on $CO_2$ earth degassing. Nat. Commun. 9, 4608. https://doi.org/10.1038/s41467-018-07087-z.
Tao, M., 2005. Characteristics of mantle degassing and deep-seated geological structures in different typical fault zones of China. Sci. China Ser. D-Earth Sci. 48 (7), 1074–1088.
Wang, W.H., 2008. The Study of the Relationship between the Characteristics of the Deep Fluid and the Regional Seismic Activity in the Northern Margin Fault Zone of the Qinling. Lanzhou Institute of Seismology, China Earthquake Administration, Lanzhou. https://doi.org/10.1016/j.epsl.2008.12.038 (in Chinese with an English abstract).
Wang, M., Shen, Z.K., 2019. Present-day crustal deformation of continental China derived from GPS and its tectonic implications. J. Geophys. Res.-Solid Earth 125 (2). https://doi.org/10.1029/2019 JB018774.
Wang, F., Zhang, B., 1991. The Relation between the contents of rare-gases and trace-elements in hot springs and tectonic actives in the eastern GanSu province. Northwest. Seismol. J. 13 (4), 14–21 (in Chinese with an English abstract).
Wang, Jun, Liu, Q., Chen, J., Cheng, L.S., Guo, B., Li, Y., 2009. Three-dimensional S-wave velocity structure of the crust and upper mantle beneath the Capital Circle Region from receiver function inversion. Chin. J. Geophys. 52 (10), 2472–2482. https://doi.org/10.3969/j.issn.0001-5733.2009.10.006 (in Chinese with an English abstract).
Weiss, R.F., 1971. Solubility *of* helium and neon in water and seawater. J. Chem. Eng. Data 16 (2), 235–241. https://doi.org/10.1021/je60049a019.
Wu, F.Y., Lin, J.Q., Wilde, S.A., Yang, J.H., 2005. Nature and significance of the Early Cretaceous giant igneous event in eastern China. Earth Planet. Sci. Lett. 233 (1–2), 103–119. https://doi.org/10.1016/j.epsl.2005.02.019.
Wu, P., Ding, Z., Tan, H., Yang, Q., Wang, X., 2021. Inversion MT data for the electrical structure beneath the Zhangbo seismic belt based on constraint of the $V_P/V_S$ model. Chin. J. Geophys. 64 (8), 2716–2732. https://doi.org/10.6038/cjg2021O0292 (in Chinese with an English abstract).
Xu, S., Zheng, G., Wang, X., Wang, H., Nakai, S., Wakita, H., 2014. Helium and carbon isotope variations in Liaodong Peninsula, NE China. J. Asian Earth Sci. 90, 149–156. https://doi.org/10.1016/j.jseaes.2014.04.019.
Yang, Y., Li, Y., Guan, Z.J., Chen, Z., Zhang, L., Lv, C.J., Sun, F.X., 2018. Correlations between the radon concentrations in soil gas and the activity of the Anninghe and the Zemuhe faults in Sichuan, southwestern of China. Appl. Geochem. 89, 23–33. https://doi.org/10.1016/j.apgeochem.2017.11.006.
Yuce, G., Italiano, F., D'Alessandro, W., Yalcin, T.H., Yasin, D.U., Gulbay, A.H., Ozyurt, N.N., Rojay, B., Karabacak, V., Bellomo, S., Brusca, L., Yang, T.F., Fu, C.C., Lai, C.W., Ozacar, A., Walia, V., 2014. Origin and interactions of fluids circulating over the Amik Basin (Hatay-Turkey) and relationships with the hydrologic, geologic and tectonic settings. Chem. Geol. 388, 23–39. https://doi.org/10.1016/j.chemgeo.2014.09.006.
Yuce, G., Fu, C., D'Alessandro, W., Gulbay, A., Lai, C., Bellomo, S., Yang, T., Italiano, F., Walia, V., 2017. Geochemical characteristics of soil radon and carbon dioxide within the Dead Sea fault and Karasu fault in the Amik basin (Hatay), Turkey. Chem. Geol. 469, 129–146. https://doi.org/10.1016/j.chemgeo.2017.01.003.
Zeng, G., He, Z.Y., Li, Z., Xu, X.S., Chen, L.H., 2016. Geodynamics of paleo-Pacific plate subduction constrained by the source lithologies ofLate Mesozoic basalts in southeastern China. Geophys. Res. Lett. 43 (19), 10189–10197. https://doi.org/10.1002/2016GL070346.
Zhai, M., 2019. Tectonic evolution of the North China Craton. J. Geom. 25 (5), 722–745. https://doi.org/10.12090/j.issn.1006-6616.2019.25.05.063 (in Chinese with an English abstract).
Zhai, M., Liu, W., 2003. Paleoproterozoic tectonic history of the North China craton: a review. Precambrian Res. 122 (1–4), 183–199. https://doi.org/10.1016/S0301-9268(02)00211-5.
Zhai, M., Santosh, M., 2013. Metallogeny of the North China Craton: link with secular changes in the evolving Earth. Gondwana Res. 24 (1), 275–297. https://doi.org/10.1016/j.gr.2013.02.007.
Zhan, Y., Yang, H., Zhao, G., Zhao, Q., Sun, X., 2017. Deep electrical structure of crust beneath the Madongshan step area at the Haiyan fault in the northeastern margin of the Tibetan plateau and tectonic implications. Chin. J. Geophys.-Chin. Ed. 60 (6), 2371–2384. https://doi.0.6038/cjg2017062.
Zhang, L., Wang, C., Cao, K., Wang, Q., Tan, J., Gao, Y., 2016. High elevation of Jiaolai Basin during the Late Cretaceous: implication for the coastal mountains along the East Asian margin. Earth Planet. Sci. Lett. 456, 112–123. https://doi.org/10.1016/j.epsl.2016.09.034.
Zhang, Y.G., Zheng, W.J., Wang, Y.J., Zhang, D.L., Tian, Y.T., Wang, M., Zhang, Z.Q., Zhang, P.Z., 2018. Contemporary deformation of the North China plain from global positioning system data. Geophys. Res. Lett. 45 (4), 1851–1859. https://doi.org/10.1002/2017GL076599.
Zhang, M., Guo, Z., Xu, S., Barry, P.H., Sano, Y., Zhang, L., Halldórsson, S.A., Chen, A.T., Cheng, Z., Liu, C.Q., Li, S.L., Lang, Y.C., Zheng, G., Li, Z., Li, L., Li, Y., 2021. Linking deeply-sourced volatile emissions to plateau growth dynamics in southeastern Tibetan Plateau. Nat. Commun. 12, 4157. https://doi.org/10.1038/s41467-021-24415-y.
Zhao, Y., Zhai, M., Chen, H., Zhang, S., 2017. Paleozoic-early Jurassic tectonic evolution of North China Craton and its adjacent orogenic belts. Geol. China 44 (1), 44–60. https://doi.org/10.12029/gc20170104.
Zhao, P., Chen, J., Li, Y., Liu, Q., Chen, Y., Guo, B., Yin, X., 2021. Growth of the northeastern Tibetan Plateau driven by crustal channel flow: evidence from high-resolution ambient noise imaging. Geophys. Res. Lett. 48 (13) https://doi.org/10.1029/2021GL093387 e2021GL093387.
Zheng, T., Zhao, L., Zhu, R., 2009. New evidence from seismic imaging for subduction during assembly of the North China craton. Geology 37 (5), 395–398. https://doi.org/10.1130/G25600A.1.
Zheng, T.Y., He, Y.M., Yang, J.H., Zhao, L., 2015. Seismological constraints on the crustal structures generated by continental rejuvenation in northeastern China. Sci. Rep. 5 (1), 1–8. https://doi.org/10.1038/srep14995.
Zhou, X.C., Wang, C.Y., Chai, C.Z., Si, X.Y., Lei, Q.Y., Li, Y., Xie, C., Liu, S.C., 2011. The geochemical characteristics of soil gas in the southeastern part of Haiyuan fault. Seismol. Geol. 33 (1), 123–132. https://doi.org/10.3969/j.issn.0253-4967.2011.01.012 (in Chinese with an English abstract).
Zhu, R., Xu, Y., Zhu, G., Zhang, H., Xia, Q., Zheng, T., 2012. Destruction of the North China craton. Sci. China-Earth Sci. 55 (10), 1565–1587. https://doi.org/10.1007/s11430-012-4516-y.